

# Magnetic-field-induced helical and stripe phases in Rashba superconductors

D. F. Agterberg and R. P. Kaur

*Department of Physics, University of Wisconsin-Milwaukee, Milwaukee, Wisconsin 53211, USA*

(Received 7 December 2006; published 23 February 2007)

Due to the lack of both parity and time-reversal symmetries, the Rashba superconductors CePt<sub>3</sub>Si, CeRhSi<sub>3</sub>, and CeIrSi<sub>3</sub>, in the presence of a magnetic field, are unstable to helical (single plane wave) order. We develop a microscopic theory for such superconductors and examine the stability of this helical phase. We show that the helical phase typically occupies most of the magnetic field–temperature phase diagram. However, we also find that this phase is sometimes unstable to a multiple- $q$  phase (loosely called a stripe phase), in which both the magnitude and the phase of the order parameter are spatially varying. We find the position of this helical to multiple- $q$  phase transition. We further examine the density of states and identify features unique to the helical phase.

DOI: [10.1103/PhysRevB.75.064511](https://doi.org/10.1103/PhysRevB.75.064511)

PACS number(s): 74.20.-z, 71.18.+y, 74.70.Tx

## I. INTRODUCTION

Recently, a class of heavy fermion superconductors has been found to break parity symmetry.<sup>1–3</sup> The broken parity symmetry implies that the three materials CePt<sub>3</sub>Si, CeRhSi<sub>3</sub>, and CeIrSi<sub>3</sub> all allow a Rashba spin-orbit coupling. The energy scale of this coupling is much larger than the superconducting energy scale.<sup>4,5</sup> This has many nontrivial implications on the resulting superconducting state.<sup>6–18</sup> Of particular relevance to the work presented here are the unusually high upper critical fields in these three Rashba superconductors. These fields substantially exceed the usual Pauli limiting field. Consequently, the Zeeman interaction must play an important role in the physics of the superconducting state. Some progress has been made in identifying the ground states of Rashba superconductors in Zeeman fields. In particular, microscopic arguments have been presented that indicate that a superconducting “stripe” phase appears in two-dimensional (2D)  $s$ -wave Rashba superconductors when a Zeeman field is applied in the plane.<sup>9,11</sup> This phase resembles the Zeeman field induced phase for conventional superconductors found theoretically by Fulde, Ferrell, Larkin, and Ovchinnikov<sup>19,20</sup> (FFLO) and which has recently been observed in CeCoIn<sub>5</sub>.<sup>21,22</sup> In the FFLO phase, the superconducting order vanishes periodically along a line, taking the simple form  $\Delta(\mathbf{R}) = \Delta_0 \cos(\mathbf{q} \cdot \mathbf{R})$  near the upper critical field. As the field is reduced, more Fourier components appear in the order parameter of this phase and, at low enough fields, a true stripelike order develops.<sup>20</sup> We will call this phase (and its appropriate generalization to Rashba superconductors) the multiple- $q$  phase. However, phenomenological arguments for Rashba superconductors indicate that a helical phase is the stable ground state near  $T_c$  once a magnetic field is applied.<sup>8,16,17</sup> In this phase, the order parameter takes the form  $\Delta(\mathbf{R}) = \Delta_0 e^{i\mathbf{q} \cdot \mathbf{R}}$ . The gap magnitude is spatially homogeneous and therefore the helical phase exhibits quite different physical properties than that of the multiple- $q$  phase. To address the physical properties of Rashba superconductors in magnetic fields, it is important to understand which of these phases are stabilized.

Vortices will also play an important role in understanding the physics of Rashba superconductors in magnetic fields.

This work focuses on the role of a Zeeman field on Rashba superconductors. Previous experience has shown that the physics associated with the Zeeman field persists when vortices are present. In particular, the Zeeman field induced FFLO phase coexists with vortices in the heavy fermion superconductor CeCoIn<sub>5</sub>.<sup>21,22</sup> Furthermore, the helical phase discussed above has been shown to coexist with vortices in Rashba superconductors near the upper critical field.<sup>16,17</sup>

To understand the microscopic origin of the helical and multiple- $q$  phases, it is useful to consider the quasiparticle states when inversion symmetry is broken and a Zeeman field is applied. Broken inversion symmetry allows an anti-symmetric spin-orbit coupling:  $\alpha \mathbf{g}(\mathbf{k}) \cdot \mathbf{S}_k$  for a quasiparticle with spin  $\mathbf{S}_k$  and momentum  $\mathbf{k}$ . Note that  $\mathbf{g}_k = -\mathbf{g}_{-k}$  due to time-reversal invariance. For a Rashba interaction,  $\mathbf{g}_k = (k_y, -k_x, 0)/k_F$ . The addition of the Zeeman field leads to the additional coupling  $\mu_B \mathbf{H} \cdot \mathbf{S}_k$ , and the quasiparticle energy eigenvalues become  $E_{k,\pm} = \xi_k \pm |\alpha \mathbf{g}_k + \mu_B \mathbf{H}|$ , where  $\xi_k$  is the quasiparticle energy when  $\alpha = \mu_B H = 0$ . We are interested in Zeeman fields that are comparable to the gap energy scale and therefore consider the limit  $\alpha \gg \mu_B H$ . For a cylindrical Fermi surface, with a Rashba interaction, applying a field along the  $\hat{x}$  direction, we find  $E_{k,\pm} = k_x^2/2m + (k_y \pm q/2)^2/2m \pm |\alpha \mathbf{k}|/k_F$ , where  $q = 2m\mu_B H/|\mathbf{k}|$ . The key point is that the Fermi surfaces remain circular and the centers of the two Fermi surfaces are shifted along  $\hat{y}$  in opposite directions. In this situation, one of the bands can gain condensation energy by pairing fermions through the new center of the appropriate Fermi surface. This leads to the helical phase in which the condensate wave function becomes  $\Delta(\mathbf{R}) = \Delta_0 \exp(i\mathbf{q} \cdot \mathbf{R})$ . This situation is depicted in Fig. 1. However, the gain in condensation energy of one Fermi surface is accompanied by a corresponding loss in condensation energy on the other Fermi surface, since the centers are shifted in opposite directions. This leads to a competition between the stability of the helical phase and that of the multiple- $q$  phase (in which both  $\pm \mathbf{q}$  gap function modes appear). In this paper, we address the resulting phase diagram by developing the quasiclassical Eilenberger equations for a Rashba superconductor in the limit  $\alpha \gg \mu_B H$ . We further examine the density of states of the helical phase.

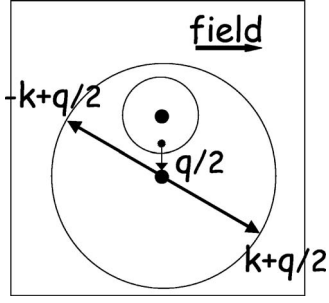


FIG. 1. A magnetic field directed as shown shifts the center of the two Fermi surfaces by  $\pm q/2$ . The smaller dot represents the point (0,0) (center of Fermi surfaces without field) and the two larger dots represent the points (0,  $-q/2$ ) and (0,  $q/2$ ) (these are the centers of the new Fermi surfaces). To gain condensation energy, pairing occurs between states of  $\mathbf{k}+q/2$  and  $-\mathbf{k}+q/2$ , leading to a gap function that has a spatial variation  $\Delta(\mathbf{R})=\Delta_0 \exp(i\mathbf{q}\cdot\mathbf{R})$ .

## II. MICROSCOPIC FORMULATION

We consider the following Hamiltonian:

$$\begin{aligned} \mathcal{H}_0 = & \sum_{k,s,s'} c_{k,s}^\dagger \{ \xi_k \sigma_0 + [\alpha \mathbf{g}_k + \mu_B \mathbf{H}] \cdot \boldsymbol{\sigma} \}_{ss'} c_{k,s'} \\ & + \frac{1}{2} \sum_{k,k',q} V(\mathbf{k}, \mathbf{k}') c_{k+q/2, \uparrow}^\dagger c_{-k+q/2, \downarrow}^\dagger c_{-k'+q/2, \downarrow} c_{k'+q/2, \uparrow}. \end{aligned} \quad (1)$$

We also set  $\langle \mathbf{g}_k^2 \rangle = 1$ , where  $\langle \rangle$  represents an average over the Fermi surface. We have restricted ourselves to spin-singlet pairing interactions since this is sufficient to capture the different physics associated with the helical phase. In the large  $\alpha$  limit,  $\alpha \gg T_c$ , the pairing problem becomes a real two-band problem in the diagonal spinor ( $\pm$ ) basis. In this basis, the pairing interaction becomes (this is after redefining the gap functions and the anomalous propagators by a  $\mathbf{k}$  dependent phase factor<sup>15</sup>)

$$V = \frac{1}{2} V(\hat{\mathbf{k}}, \hat{\mathbf{k}}') \begin{pmatrix} 1 & -1 \\ -1 & 1 \end{pmatrix}. \quad (2)$$

We work within the quasiclassical approximation and define the usual Green's functions in Nambu space for each band  $\Psi_\pm^\dagger(\mathbf{R}) = [\psi_\pm^\dagger(\mathbf{R}), \psi_\pm(\mathbf{R})]$ , and define the imaginary time Green's function

$$\hat{G}_\pm(\mathbf{x}_1, \mathbf{x}_2; \tau_1 - \tau_2) = -\langle T_\tau \Psi_\pm(\mathbf{x}_1, \tau_1) \Psi_\pm^\dagger(\mathbf{x}_2, \tau_2) \rangle, \quad (3)$$

where the operator  $T_\tau$  arranges the field operators in ascending order of the imaginary time  $0 < \tau < 1/T$  and  $\Psi(\mathbf{x}, \tau) = e^{\tau H} \Psi(\mathbf{x}) e^{-\tau H}$ . We introduce the center-of-mass coordinate  $\mathbf{R} = (\mathbf{x}_1 + \mathbf{x}_2)/2$  and the relative coordinate  $\mathbf{r} = \mathbf{x}_1 - \mathbf{x}_2$ , and perform the Fourier transformation in the latter according to

$$\hat{G}_\pm(\mathbf{k}, \mathbf{R}; \omega_n) = \int d\mathbf{r} \int_0^{1/T} d\tau \hat{G}_\pm(\mathbf{x}_1, \mathbf{x}_2; \tau) e^{-i(\mathbf{k}\cdot\mathbf{r} - \omega_n \tau)}, \quad (4)$$

where  $\omega_n = (2n+1)\pi T$  is the fermionic Matsubara frequency. We define

$$\hat{g}_\pm(\hat{\mathbf{k}}, \mathbf{R}, \omega_n) = \begin{pmatrix} g_\pm & f_\pm \\ f_\pm^\dagger & -g_\pm \end{pmatrix} \equiv \frac{i}{\pi} \int d\xi \hat{\tau}_3 \hat{G}_\pm(\mathbf{k}, \mathbf{R}, \omega_n), \quad (5)$$

where  $d\xi$  integrates out the variable perpendicular to the Fermi surface,  $\hat{\mathbf{k}}$  is a vector on the Fermi surface, and  $\tau_3$  is the  $z$  component of the Pauli matrices acting on the particle-hole space. The standard quasiclassical approach<sup>23-25</sup> results in the following Eilenberger equations for this system:

$$\left[ \omega_n \pm i\mu_B \hat{\mathbf{g}}_{\hat{\mathbf{k}}} \cdot \mathbf{B} + \mathbf{v}_{\hat{\mathbf{k}}} \cdot \left( \nabla + \frac{2ie}{c} \mathbf{A} \right) \right] f_\pm = \Delta_\pm(\hat{\mathbf{k}}, \mathbf{R}) g_\pm, \quad (6)$$

$$\left[ \omega_n \pm i\mu_B \hat{\mathbf{g}}_{\hat{\mathbf{k}}} \cdot \mathbf{B} + \mathbf{v}_{\hat{\mathbf{k}}} \cdot \left( \nabla - \frac{2ie}{c} \mathbf{A} \right) \right] f_\pm^\dagger = \Delta_\pm^*(\hat{\mathbf{k}}, \mathbf{R}) g_\pm, \quad (7)$$

where  $f_\pm^\dagger f_\pm + g_\pm^2 = 1$ ,  $\omega_n = \pi T(2n+1)$ ,  $\hat{\mathbf{k}}$  denotes  $\mathbf{k}$  restricted to the Fermi surface,  $\mathbf{A}$  is the vector potential (included for completeness), and  $\mathbf{B} = \nabla \times \mathbf{A}$ . We will neglect  $\mathbf{A}$  and set  $\mathbf{B} = \mathbf{H}$  in the following. Note that the derivation of Eqs. (6) and (7) ignores small regions in phase space where  $\mathbf{g}(\mathbf{k})$  might vanish. With the two-band pairing interaction of Eq. (2), the gap equation is

$$\Delta_i(\hat{\mathbf{k}}, \mathbf{R}) = -\pi T \sum_{n,j} N_j \langle V_{ij}(\hat{\mathbf{k}}, \hat{\mathbf{k}}') f_j(\hat{\mathbf{k}}', \mathbf{R}, \omega_n) \rangle_{\hat{\mathbf{k}}}, \quad (8)$$

where  $N_j$  is the density of states on band  $j$ . We also express  $V(\hat{\mathbf{k}}, \hat{\mathbf{k}}') = -V \varphi_\Gamma(\hat{\mathbf{k}}) \varphi_\Gamma^*(\hat{\mathbf{k}}')$ , where  $\Gamma$  labels the one-dimensional gap representation we are interested in. The gap function can be written in the product form  $\Delta_\alpha(\hat{\mathbf{k}}, \mathbf{R}) = \tilde{\Delta}_\alpha(\mathbf{R}) \varphi_\Gamma(\hat{\mathbf{k}})$ , where Eq. (2) implies that  $\tilde{\Delta}_+(\mathbf{R}) + \tilde{\Delta}_-(\mathbf{R}) = 0$ , indicating that the gap magnitudes on the two bands are equal at every position in space. Henceforth we set  $\Delta(\mathbf{R}) = -\tilde{\Delta}_+(\mathbf{R}) = \tilde{\Delta}_-(\mathbf{R})$ .

The Eilenberger equations can be derived from a Gibbs free-energy functional.<sup>23</sup> We will require this free energy to compare the energies of the different phases. Once Eqs. (6) and (7) are solved for a given functional form of  $\Delta(\mathbf{R})$ , this free-energy functional becomes

$$\Omega_{\text{SN}} = \int d\mathbf{R} \left[ V^{-1} |\Delta(\mathbf{R})|^2 - \pi T \sum_{n,j} N_j \langle I_j(\hat{\mathbf{k}}, \mathbf{R}, \omega_n) \rangle \right], \quad (9)$$

with

$$I_j(\hat{\mathbf{k}}, \mathbf{R}, \omega_n) = \frac{\varphi_\Gamma^*(\hat{\mathbf{k}}) \Delta^*(\mathbf{R}) f_j(\hat{\mathbf{k}}, \mathbf{R}, \omega_n) + f_j^\dagger(\hat{\mathbf{k}}, \mathbf{R}, \omega_n) \Delta(\mathbf{R}) \varphi_\Gamma(\hat{\mathbf{k}})}{1 + \frac{\omega_n}{|\omega_n|} g_j(\hat{\mathbf{k}}, \mathbf{R}, \omega_n)}. \quad (10)$$

## III. ANALYSIS OF THE HELICAL PHASE

### A. Helical phase solution

Equations (6) and (7) can be solved for  $\Delta(\hat{\mathbf{k}}, \mathbf{R}) = \Delta \varphi_\Gamma(\hat{\mathbf{k}}) e^{i\mathbf{q}\cdot\mathbf{R}}$  with the following solutions:

$$g_{\pm} = \frac{\tilde{\omega}_{n\pm}}{\sqrt{\tilde{\omega}_{n\pm}^2 + |\Delta\varphi_{\Gamma}(\hat{\mathbf{k}})|^2}} \quad (11)$$

and

$$f_{\pm} = \frac{\Delta\varphi_{\Gamma}(\hat{\mathbf{k}})e^{iq\cdot\mathbf{R}}}{\sqrt{\tilde{\omega}_{n\pm}^2 + |\Delta\varphi_{\Gamma}(\hat{\mathbf{k}})|^2}}, \quad (12)$$

where  $\tilde{\omega}_{n\pm} = \omega_n \pm i\mu_B \hat{\mathbf{g}} \cdot \mathbf{H} + iv \cdot \mathbf{q}$ . The free energy Eq. (9) is then minimized with respect to  $\Delta$  and  $\mathbf{q}$  to find the  $H$ - $T$  phase diagram. This phase diagram depends strongly on field orientation, dimensionality, and the relative values of  $N_-$  and  $N_+$ . It depends weakly on the pairing symmetry. For field parallel to  $\hat{z}$ , the stable state is given by  $\mathbf{q}=0$  and the physics is independent of the Zeeman field.<sup>17</sup> In the following, we consider only magnetic fields applied perpendicular to  $\hat{z}$ . When  $N_+ \neq N_-$ , then  $\mathbf{q} \neq 0$  whenever  $\mathbf{H} \neq 0$ . Some analytical results can be found for the upper critical field. For a 2D cylindrical Fermi surface, independent of pairing symmetry, the upper critical field diverges as  $T \rightarrow 0$  and  $v_F \mathbf{q} = \mu_B \hat{z} \times \mathbf{H}$  at  $H_{c2}$  for  $N_+ > N_-$  (a related result has been found previously<sup>9,11</sup>). We have further found that if both attractive spin-triplet and attractive isotropic spin-singlet pairing interactions are included, then the divergence of  $H_{c2}$  occurs at  $T > 0$  for a 2D cylindrical Fermi surface. In particular, if  $N_+ = N_-$ , then this divergence occurs when  $T = \sqrt{T_s T_p}$ , where  $T_s$  ( $T_p$ ) is the usual  $T_c$  for isotropic  $s$ -wave ( $p$ -wave) pairing when  $\alpha=0$ . For an isotropic  $s$ -wave superconductor, with a three-dimensional (3D) spherical Fermi surface at  $T=0$ ,  $H_{c2} = 2H_p e^{1+\pi|\delta N|/2}$ , where  $\delta N = (N_+ - N_-)/(N_+ + N_-)$ ,  $H_p = \Delta_0/\sqrt{2}\mu_B$  is the usual Pauli paramagnetic field, and  $\Delta_0 = 1.76T_c$ . Generically, the appearance of the helical phase enhances the upper critical field well beyond the Pauli limiting field as is observed in CePt<sub>3</sub>Si,<sup>17,26</sup> CeIrSi<sub>3</sub>,<sup>3</sup> and CeRhSi<sub>3</sub>.<sup>2</sup>

### B. Stability of the helical phase

As explained in the Introduction, there are physical reasons to suggest that the helical phase is not always stable. To

examine this possibility, we set  $\Delta(\mathbf{R}) = \Delta_q e^{iq\cdot\mathbf{R}} + \Delta_p e^{ip\cdot\mathbf{R}} + \Delta_{2q-p} e^{i(2q-p)\cdot\mathbf{R}}$ , where  $\mathbf{q}$  is the Fourier component that optimizes the helical phase free energy. The other two Fourier modes represent the instability of the helical phase to a phase we name the multiple- $q$  phase. With this solution for  $\Delta(\mathbf{R})$ , we solve Eqs. (6) and (7) perturbatively and expand the free energy in Eq. (9) to second order in these two modes.

To carry out this procedure, we rewrite the Eilenberger equations in terms of Fourier components. In particular, we set  $\Delta(\mathbf{R}) = \sum_q e^{iq\cdot\mathbf{R}} \Delta_q$ ,  $g(\mathbf{R}) = \sum_q e^{iq\cdot\mathbf{R}} g_q$ , and  $f(\mathbf{R}) = \sum_q e^{iq\cdot\mathbf{R}} f_q$  (we have suppressed the  $\alpha$ ,  $\hat{\mathbf{k}}$ , and  $\omega_n$  labels for notational simplicity). The Eilenberger equations become

$$\omega_q f_q = \sum_p \Delta_p g_{q-p}, \quad (13)$$

$$\omega_{-q} f_q^\dagger = \sum_p \Delta_p^* g_{q+p}, \quad (14)$$

$$\sum_q [g_{q+p} g_{-q} + f_{q+p} f_{-q}^\dagger] = \delta_{p,0}, \quad (15)$$

where we have defined  $\omega_q = \omega_n \pm i\mu_B \hat{\mathbf{g}} \cdot \mathbf{B} + iv \hat{\mathbf{k}} \cdot \mathbf{q}$  (the  $\pm$  refer to the two different bands). We wish to solve these equations as a perturbation about the helical phase  $\Delta_Q \neq 0$  (we use gauge invariance to choose this real), keeping terms in the free energy up to second order in  $\Delta_q$  and  $\Delta_{2Q-q}$ . To carry this out, we require  $f_q$ ,  $f_{-q}^\dagger$ ,  $g_{q-Q}$ , and  $g_{Q-q}$  to first order in the perturbation and  $g_0$  and  $f_Q + f_{-Q}^\dagger$  to second order in the perturbation. We label the second order corrections to  $g_0$ ,  $f_Q + f_{-Q}^\dagger$  as  $\tilde{g}_0$ ,  $\tilde{f}_Q + \tilde{f}_{-Q}^\dagger$  and keep the labels  $g_0$ ,  $f_Q$ ,  $f_{-Q}^\dagger$  for the zeroth order perturbation. A lengthy calculation gives

$$f_q = \frac{g_0 [(2\omega_Q \omega_{2Q-q} + \Delta_Q^2) \Delta_q - \Delta_Q^2 \Delta_{2Q-q}^*]}{2\omega_Q \omega_q \omega_{2Q-q} + \Delta_Q^2 (\omega_q + \omega_{2Q-q})}, \quad (16)$$

$$g_{q-Q} = -\frac{g_0 \Delta_Q [\omega_{2Q-q} \Delta_q + \omega_q \Delta_{2Q-q}^*]}{2\omega_q \omega_{2Q-q} \omega_Q + \Delta_Q^2 (\omega_q + \omega_{2Q-q})}, \quad (17)$$

$$\tilde{f}_Q + \tilde{f}_{-Q}^\dagger = \frac{g_0 g_{q-Q} (\Delta_q + \Delta_{2Q-q}^*) + g_0 g_{q-Q} (\Delta_q^* + \Delta_{2Q-q}) - 2\Delta_Q g_{q-Q} g_{Q-q} - f_{-q}^\dagger f_q \Delta_Q - f_{-2Q+q}^\dagger f_{2Q-q} \Delta_Q}{g_0 \omega_Q + \Delta_Q f_Q}, \quad (18)$$

and

$$\tilde{g}_0 = -\frac{2g_{q-Q} g_{Q-q} + f_Q (\tilde{f}_Q + \tilde{f}_{-Q}^\dagger) + f_{-q}^\dagger f_q + f_{-2Q+q}^\dagger f_{2Q-q}}{2g_0}. \quad (19)$$

Using these expressions in Eq. (9) leads to a free energy of the form

$$\alpha_p |\Delta_p|^2 + \alpha_{2q-p} |\Delta_{2q-p}|^2 + \alpha_m \Delta_p \Delta_{2q-p} + \alpha_m^* \Delta_p^* \Delta_{2q-p}^*. \quad (20)$$

The helical phase is unstable when the above free energy becomes negative for any choice of  $\Delta_p$  or  $\Delta_{2q-p}$ . We find numerically that the instability occurs for  $\mathbf{p} = -\mathbf{q}$ . Figure 2 shows the phase diagram found for  $N_+ = N_-$  ( $\delta N = 0$ ) for isotropic pairing with a 3D spherical Fermi surface. In this case,

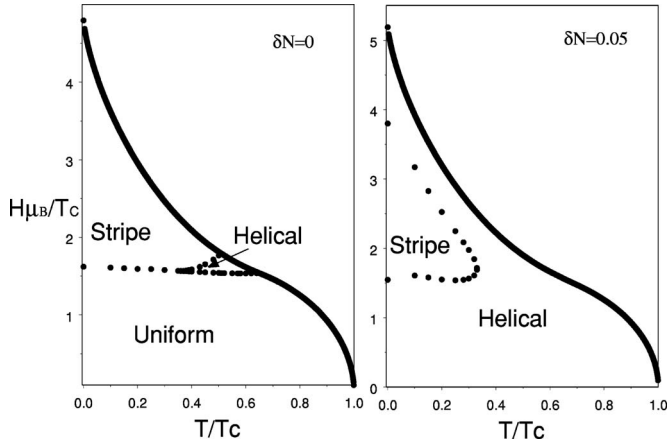


FIG. 2. Phase diagram for an isotropic  $s$ -wave superconductor with a 3D spherical Fermi surface when  $\delta N=0$  and  $\delta N=0.05$ . When  $N_+$  and  $N_-$  differ slightly, the helical phase dominates the phase diagram. Stripe denotes the multiple- $q$  phase.

the helical phase occupies only a small region of the phase diagram. We find that the transition from the uniform phase into the helical phase is first order for  $T/T_c < 0.39$ . However, for  $T < 0.36$ , we find that the helical phase is itself unstable to the multiple- $q$  phase. Figure 2 also shows the phase diagram found when  $\delta N=0.05$ . Contrary to  $\delta N=0$ , the helical phase occupies almost the entire phase diagram, with the multiple- $q$  phase existing in a region at low temperature and moderate fields. The region occupied by the multiple- $q$  phase decreases as  $\delta N$  increases. Once  $\delta N > 0.25$ , we find that the multiple- $q$  phase ceases to exist. The suppression of the multiple- $q$  phase due to an increasing  $\delta N$  occurs for all pairing symmetries. It would nevertheless be of interest to look for the helical to multiple- $q$  phase transition in Rashba superconductors. Fujimoto has pointed out that Fermi liquid corrections for heavy fermion materials lead to a large enhancement of a magnetoelectric effect that has the same origin as the helical phase.<sup>17,18</sup> In our theory, this enhancement is captured by an increase of  $\delta N$ .

### C. Density of states in the helical phase

Having established the stability of the helical phase, it is of interest to determine some of its physical properties. The density of states  $N(\omega)$  is an important quantity for many properties and it is given by

$$N(\omega) = \sum_{j=\pm} N_j \Re \left\langle \frac{|\tilde{\omega}_j|}{\sqrt{\tilde{\omega}_j^2 - |\Delta \varphi_{\Gamma}(\hat{\mathbf{k}})|^2}} \right\rangle_{\hat{\mathbf{k}}}, \quad (21)$$

where  $\tilde{\omega}_{\pm} = \omega \pm \mu_B \hat{\mathbf{g}}_{\hat{\mathbf{k}}} \cdot \mathbf{H} + v_{\hat{\mathbf{k}}} \cdot \mathbf{q}$ . Here we consider in detail  $d_{x^2-y^2}$  pairing symmetry on a 2D cylindrical Fermi surface at  $T/T_c=0.15$  (and give analogous results for isotropic  $s$ -wave pairing). Note that  $d_{x^2-y^2}$  pairing is a possible pairing symmetry in CePt<sub>3</sub>Si, in which line nodes have been observed.<sup>27,28</sup> We set  $\delta N=0.25$  and have checked that the helical phase is the stable ground state. For  $T/T_c=0.15$ ,  $H_{c2}=21H_P$  with the field applied along the gap maxima. The evolution of  $N(\omega)$  reveals two properties of interest that are

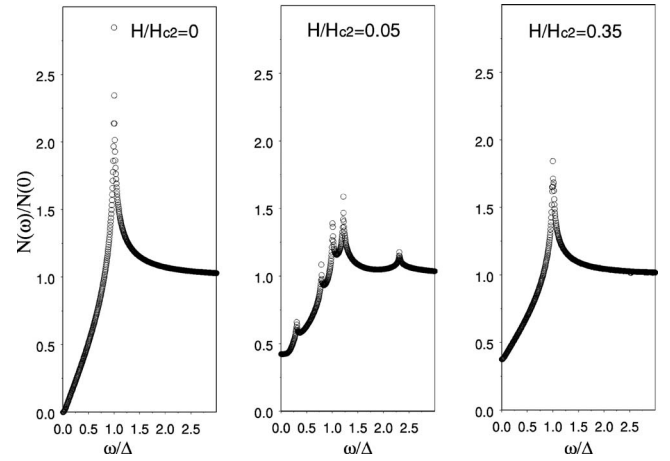


FIG. 3. Density of states in the helical phase for increasing magnetic fields for a  $d$ -wave superconductor. The high field density of states is field independent and corresponds to that of an ungapped band and a gapped band.

revealed in Fig. 3. The most significant property is that for fields  $H/H_{c2} \geq \approx 0.25$ ,  $N(\omega)$  is field independent and has two contributions. The first is a normal component that exists on one of the bands, and the second contribution is the usual  $d$ -wave density of states from the second band. Similar behavior exists for isotropic  $s$ -wave pairing as is shown in Fig. 4. The observation that  $N(\omega)$  for one of the bands corresponds to that of a normal metal is intriguing because it exists even though both bands have the same pairing amplitudes. Nevertheless, this result is intuitive because one band prefers  $v_F \mathbf{q} = \mu_B \hat{\mathbf{z}} \times \mathbf{H}$  and is not frustrated, while the other band prefers  $v_F \mathbf{q} = -\mu_B \hat{\mathbf{z}} \times \mathbf{H}$  and therefore cannot pair the fermions that are on the Fermi surface. This manifests itself as an increase of  $N(\omega)$ . It is natural to expect that the frustrated band will have its gap amplitude become zero at sufficiently large fields. This possibility is not permitted by the theory considered here because only spin-singlet pairing interactions have been included. Introducing an attractive spin-triplet pairing interaction will lead to a gap that vanishes on

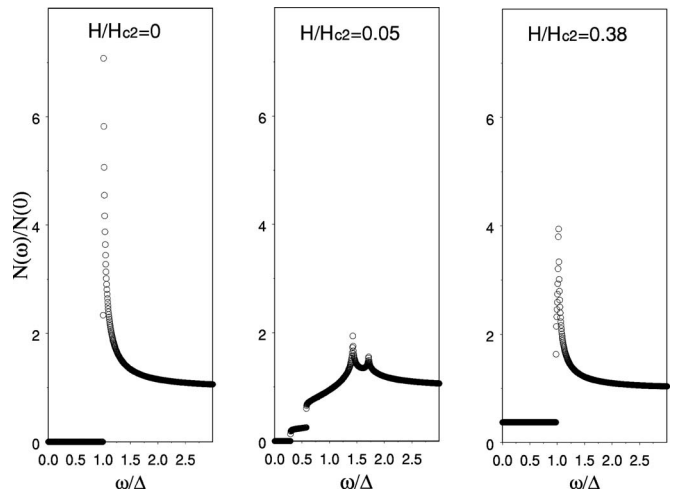


FIG. 4. Density of states in the helical phase for increasing magnetic fields for an  $s$ -wave superconductor.

the frustrated band as the field is increased. However, even if the frustrated band has zero gap amplitude, the single particle density of states will remain qualitatively the same.

The second property of interest occurs at low fields. In particular, the single peak at  $\omega=\Delta$  of the  $H=0$  density of states splits into five peaks: one at  $\omega=\Delta$  and the others at approximately  $\omega=|\Delta\pm\mu_B H\pm v_F q|$ . This occurs for the field applied along the directions in which the gap is maximal. This property is anisotropic; for the field applied along the gap nodes, the  $\omega=\Delta$  peak splits into four features that occur at approximately  $\omega=|\Delta\pm\mu_B H/\sqrt{2}\pm v_F q/\sqrt{2}|$ . This property may provide a means to probe the gap symmetry in CePt<sub>3</sub>Si. Note that if  $\mathbf{q}=0$ , then an anisotropy still exists in  $N(\omega)$ . At low fields, the  $s$ -wave density of states has four features for all in-plane field orientations as is shown in Fig. 4.

#### IV. CONCLUSIONS

We have derived the quasiclassical Eilenberger theory describing Rashba superconductors. Using this theory, we have

examined the stability of helical and multiple- $q$  phases for Rashba superconductors in magnetic fields. We have found that the helical phase is stable over a wide range of the phase diagram. Finally, we have examined the single-particle density of states in the helical phase and have revealed that at large fields it behaves qualitatively differently for the two spin-split bands. On one band, the density of states is completely normal, while on the other band it remains gapped and resembles the zero-field superconducting density of states.

#### ACKNOWLEDGMENTS

We are grateful to P. A. Frigeri, N. Hayashi, and M. Sigrist for many helpful discussions. This work was supported by the National Science Foundation Grant No. DMR-0381665.

- 
- <sup>1</sup>E. Bauer, G. Hilscher, H. Michor, C. Paul, E. W. Scheidt, A. Griбанov, Y. Seropegin, H. Noel, M. Sigrist, and P. Rogl, Phys. Rev. Lett. **92**, 027003 (2004).
- <sup>2</sup>N. Kimura, K. Ito, K. Saitch, Y. Umeda, H. Aoki, and T. Terachima, Phys. Rev. Lett. **95**, 247004 (2005).
- <sup>3</sup>I. Sugitani, Y. Okuda, H. Shishido, T. Yamada, A. Thamizhavel, E. Yamamoto, T. D. Matsuda, Y. Haga, T. Takeuchi, R. Settai, and Y. Onuki, J. Phys. Soc. Jpn. **75**, 043703 (2006).
- <sup>4</sup>K. V. Samokhin, E. S. Zijlstra, and S. K. Bose, Phys. Rev. B **69**, 094514 (2004); **70**, 069902(E) (2004).
- <sup>5</sup>N. Kimura, Y. Umeda, T. Asai, T. Terashima, and H. Aoki, Physica B **294B-295B**, 280 (2001).
- <sup>6</sup>V. M. Edelstein, Sov. Phys. JETP **68**, 1244 (1989).
- <sup>7</sup>L. P. Gor'kov and E. I. Rashba, Phys. Rev. Lett. **87**, 037004 (2001).
- <sup>8</sup>D. F. Agterberg, Physica C **387**, 13 (2003).
- <sup>9</sup>V. Barzykin and L. P. Gor'kov, Phys. Rev. Lett. **89**, 227002 (2002).
- <sup>10</sup>S. K. Yip, Phys. Rev. B **65**, 144508 (2002).
- <sup>11</sup>O. V. Dimitrova and M. V. Feigel'man, Pis'ma Zh. Eksp. Teor. Fiz. **78**, 1132 (2003) [JETP Lett. **78**, 637 (2003)].
- <sup>12</sup>P. A. Frigeri, D. F. Agterberg, A. Koga, and M. Sigrist, Phys. Rev. Lett. **92**, 097001 (2004).
- <sup>13</sup>V. P. Mineev, Int. J. Mod. Phys. B **18**, 2963 (2004).
- <sup>14</sup>S. S. Saxena and P. Monthoux, Nature (London) **427**, 799 (2004).
- <sup>15</sup>I. A. Sergienko and S. H. Curnoe, Phys. Rev. B **70**, 214510 (2004).
- <sup>16</sup>K. V. Samokhin, Phys. Rev. B **70**, 104521 (2004).
- <sup>17</sup>R. P. Kaur, D. F. Agterberg, and M. Sigrist, Phys. Rev. Lett. **94**, 137002 (2005).
- <sup>18</sup>S. Fujimoto, Phys. Rev. B **72**, 024515 (2005).
- <sup>19</sup>P. Fulde and A. Ferrell, Phys. Rev. **135**, A550 (1964).
- <sup>20</sup>A. I. Larkin and Yu. N. Ovchinnikov, Sov. Phys. JETP **20**, 762 (1965).
- <sup>21</sup>A. Bianchi, R. Movshovich, C. Capan, P. G. Pagliuso, and J. L. Sarrao, Phys. Rev. Lett. **91**, 187004 (2003).
- <sup>22</sup>H. A. Radovan, N. A. Fortune, T. P. Murphy, S. T. Hannahs, E. C. Palm, S. W. Tozer, and D. Hall, Nature (London) **425**, 51 (2003).
- <sup>23</sup>G. Eilenberger, Z. Phys. **214**, 195 (1968).
- <sup>24</sup>A. I. Larkin and Y. N. Ovchinnikov, Zh. Eksp. Teor. Fiz. **55**, 2262 (1968) [Sov. Phys. JETP **28**, 1200 (1969)].
- <sup>25</sup>J. W. Serene and D. Rainer, Phys. Rep. **101**, 221 (1983).
- <sup>26</sup>T. Yasuda, H. Shishido, T. Ueda, S. Hashimoto, R. Settai, T. Takeuchi, T. D. Matsuda, Y. Haga, and Y. Onuki, J. Phys. Soc. Jpn. **73**, 1657 (2004).
- <sup>27</sup>K. Izawa, Y. Kasahara, Y. Matsuda, K. Behnia, T. Yasuda, R. Settai, and Y. Onuki, Phys. Rev. Lett. **94**, 197002 (2005).
- <sup>28</sup>I. Bonalde, W. Bramer-Escamilla, and E. Bauer, Phys. Rev. Lett. **94**, 207002 (2005).